

A Novel Optimal Deep Learning Based Image Retrieval and Classification Model for Biomedical Images

C. Ashok Kumar¹ and S.Sathiamoorthy^{2*}

¹ Division of Computer and Information Science, Annamalai University,
Annamalai Nagar

²Tamil Virtual Academy, Chennai,

¹cashok1976@gmail.com, ²ks_sathia@yahoo.com

Abstract

In recent times, there is an exponential growth in the generation and utilization of medical images, which offers extensive details about the anatomical structure of a patient. Therefore, medicinal images have been utilized for diagnostics and research purposes to understand the deep insight into the reason and treatment of diverse diseases. To retrieve and classify the medicinal images from huge databases, it is needed to develop an effective medical image retrieval and classification model. In this paper, a new medical image retrieval and classification model has been developed incorporating three different processes namely feature extraction, similarity measurement based image retrieval and image classification. At the earlier level, texture and shape features are extracted from the original image. On the application of new query image as input, the image retrieval process is executed utilizing a Euclidean distance based similarity measure to retrieve the relevant images. Then, grey wolf optimization (GWO) tuned deep neural network (DNN) called GWO-DNN model is applied for classification task. The hyperparameter tuning of DNN model takes place by the use of GWO algorithm. Finally, the classification process gets executed and assign class label to the applied test image. To validate the results, a benchmark NEMA CT images is utilized. The experimental results clearly portrayed the significance of the proposed model by attaining a maximum precision of 89.39%, recall of 94.18% and accuracy of 93.73%.

Keywords: — Classification, Feature extraction, Deep learning, Hyperparameter tuning, Image retrieval

1. Introduction

Recently, latest advancements in the domain of electronics, multimedia, as well as storage methods results to numerous image generation as well as multimedia databases. The clinical and diagnosing processes finds beneficial from the latest digital storage as well as content processing. Several medical firms involve medical imaging techniques for diagnosing and examining services that tends to increase clinical image count. Thus, development of effective medical image retrieving technique is more essential to help doctors to analyze huge dataset. In order to tackle numerous clinical image dataset, various methods are presented for automated medical image analysis that is carried out in [1–5]. Also, Content Based Medical Image Retrieval (CBMIR) method is effective in examining diverse types of ailments and acts as a qualified management tool [6] to manage the huge database. Without applying these techniques, accessing, tackling as well as filtering require data from numerous dataset is a complex task. The retrieval of medicinal images are based on textual data such as tags as well as manual annotations which tends to generate minimal outcome as it needs more contribution of humans, expert's investigation as well as time interval. These complexities present in the above tends to design an powerful CBMIR technique that classifies as well as retrieves the images in an automatic manner on the basis of obtained features from image. It is also

used to identify essential clinical decision support framework and find relevant data from massive repository.

Content Based Image Retrieval (CBIR) is based on computer vision that offers a process of obtaining relative images that is available in huge dataset. The exploration task depends upon the image features like color, texture shape, and alternate factors filtered from the images. The efficiency of CBIR methods are based on the selected features [7]. Here, images can be described in terms of existing features from a greater dimensional feature space. Followed by, the homogeneous attribute among the images placed in a database as well as query image has been computed in feature space through a distance value like Euclidean distance.

In recent times, a rapid growth in the field of Deep Learning (DL) techniques has been presented which is obtained from the idea of human brain [8], that stores every data regarding human brain and its operates through various layers of transformation. As a result, to learn features in an automated manner with multiple levels of abstraction, deep architectural techniques and machine learning (ML) schemes has offered a direct approach to obtain feature representation by allowing the method to learn complex features exist in the actual images without the application of hand crafted parameters.

Numerous studies have applied DL methods to classify the retrieved clinical images. In [7], classification of benign as well as malignant breast masses takes place bases on the textual parameters of sonography images. In [8], a medicinal retrieving method for Diabetic Retinopathy (DR) and mammographic images has been devised. In addition, it has been employed with a best wavelet transform including lifting approach and allocating weights for all wavelet sub-bands. Followed by, other processes are also based on the wavelet transform that helps to retrieve brain image, which is defined [9]. Therefore, co-occurrence matrix based CT and MRI image retrieval process is established in [10]. A faster local-structure-based region-of-interest (ROI) retrieval technique for brain MRI image has been offered in [11]. [12] provides a quantitative analysis for pulmonary emphysema that is identified in CT images of Local Binary Pattern (LBP). Later, it is used in a collected manner of LBP, joint LBP and the intensity histograms are characterized by region of interest (ROI). [13] developed a Uniformity Estimation Method (UEM), which is helpful to extract the local intensity as well as textures to find a pathological modification in heart computer tomography (CT) images. [14] used a method for retrieving 2-dimentional MRI images as multimodal as well as noise management. The final outcomes derived from the above models depicted that the results are effective in terms of accuracy, speed, robust, and so on.

[15] presented a feature extraction approach known as Local Co-Occurrence Ternary Patterns (LTCOP) which has been applied to encode the co-occurrence of identical ternary edges of an image. By using the central pixel, the value of LTCOP can be measured according to first order derivatives that are extracted from eight dimensions. Subsequently, filtered results show that, the superiority of projected model is powerful than alternate methodologies such as LBP, Local Directional Pattern (LDP), Local Ternary Pattern (LTP) etc. Then, practitioners have organized a feature description for retrieving biomedical image said to be Local Mesh Patterns (LMeP) [16]. Here, LMeP is employed for encoding the correlation encircled by neighbors of offered reference image which is not as same as LBP, and used for encoding the link between the predetermined reference pixels and enclosed neighbors. Hence, it has been extended in [17] to obtain LMePVEP which has LMP with valley edge patterns (VEP) to be applied. It states that LMePVEP shows an increment in terms of different measures upon comparison with LBP and corresponding variants.

[18] applied a technique termed as Local Diagonal Extrema Pattern (LDEP) for retrieving CT images. It employs the first order derivatives to calculate the metrics LDE.

Such indexes are utilized in developing the feature descriptor for overall image. For demonstrating the power and excellence of this model, researchers have related the simulation outcome along with filtered state-of-the-art approaches namely LMeP, LTCOP, LTP, CSLBP, and LBP. It depicts an improvement in precision retrieval while reducing the computation time. It also provides various benefits when compared with other models since it holds reduced dimension of feature vector, by offering maximum process by employing minimized features.

Though diverse models exist to retrieve and classify medicinal images, still there exists a requirement to develop new model. To retrieve and classify the medicinal images from huge databases, it is needed to develop an effective medical image retrieval and classification model.

The contribution of the paper is provided here. In this paper, a new medical image retrieval and classification model has been developed. The presented model incorporates feature extraction, image retrieval and image classification. At the earlier level, texture and shape features are extracted from the original image. On the application of new query image as input, the presented GWO-DNN model will extract the features and compute the similarity metric to retrieve the relevant images utilizing a Euclidean distance based similarity measure. Then, grey wolf optimization (GWO) tuned deep neural network (DNN) called GWO-DNN model for classification task. Finally, the classification process gets executed and assign class label to the applied test image. To validate the results, a benchmark NEMA CT images is utilized. A detailed experimentation is done and the outcome ensured the effective retrieval and classification performance of the presented model.

The remaining sections are arranged as follows. Section 2 provides a clear explanation of the GWO-DNN model. Section 3 offers a brief discussion of GWO-DNN and Section 4 concludes the work.

2. The proposed model

The overall tasks contributed in projected method are demonstrated in Figure 1. As given in figure, the entire process is divided into two main phases namely training phase and testing phase. In the training phase, the input image is induced to feature extraction stage which involves an extraction of a set of two definite features like texture as well as edges by applying the Directional Local Ternary Quantized Extrema Patterns (DLTerQEPs) and Zernike Moments (ZM). During the testing phase, the input query image undergo feature extraction process and attains a set of features exist in the image. Then, the resemblance among the test image and images placed in the databases has been computed in feature space under the application of Euclidean distance. Based on the similarity measure, the relevant images will be retrieved. After the retrieving of relevant images, GWO-DNN dependent image classification process is carried out. Therefore, the above described tasks are reported in the upcoming sections.

2.1. Texture feature extraction using DLTerQEP model

In this section, the DLTerQEP technique has been applied to extract the texture features present in the applied image. DLTerQEP refers to a spatial structure of ternary patterns with the help of local extrema and directional geometric structures. In DLTerQEP, the given image is comprised with local extrema for all dimensions that should be estimated using local differences between middle and neighboring pixels by the employment of pattern indexing and pixel positions. Also, the positions are indexed by using four (tetra) dimensional extremas operator calculations.

The Local Directional Extrema Values (LDEV) is applied for local patterns of an image and is estimated by the given Eq. (1):

$$LDEV(q, r) = \sum_{q=1}^{t_1} \sum_{r=1}^{t_1} [IG(q, r) - IG(1 + \text{floor}(t_1/2), 1 + \text{floor}(t_1/2))] \quad (1)$$

where, the input image has the size of $t_1 \times t_1$. The four directional, HVDA₇ structures of possible direction of LQP geometries are used in feature extraction task. The directional local extrema measures in 0°, 45°, 90°, 135° directions has been extracted in the form of HVDA₇ and filtered from LDEV valued as computed by Eq. (2). Then, 4 Directional Ternary Extrema Coding's (DTEC) are collected according to the four dimensions (0°, 45°, 90°, 135°) from various thresholds with the help of LTP model. Thus, ternary coding patterns can be derived from the given function as:

$$DTEC1(IG(gy_c))|_{\alpha} =$$

$$\left\{ \begin{array}{l} \vec{f}_2(LDEV(gy_{45}) \times LDEV(gy_{43}), IG(gy_c)); \vec{f}_2(LDEV(gy_{46}) \times LDEV(gy_{42}), IG(gy_c)); \vec{f}_2(LDEV(gy_{47}) \times LDEV(gy_{41}), IG(gy_c)); \alpha = 0^\circ \\ \vec{f}_2(LDEV(gy_{34}) \times LDEV(gy_{54}), IG(gy_c)); \vec{f}_2(LDEV(gy_{24}) \times LDEV(gy_{64}), IG(gy_c)); \vec{f}_2(LDEV(gy_{14}) \times LDEV(gy_{74}), IG(gy_c)); \alpha = 45^\circ \\ \vec{f}_2(LDEV(gy_{35}) \times LDEV(gy_{53}), IG(gy_c)); \vec{f}_2(LDEV(gy_{26}) \times LDEV(gy_{62}), IG(gy_c)); \vec{f}_2(LDEV(gy_{17}) \times LDEV(gy_{71}), IG(gy_c)); \alpha = 90^\circ \\ \vec{f}_2(LDEV(gy_{33}) \times LDEV(gy_{55}), IG(gy_c)); \vec{f}_2(LDEV(gy_{22}) \times LDEV(gy_{66}), IG(gy_c)); \vec{f}_2(LDEV(gy_{11}) \times LDEV(gy_{77}), IG(gy_c)); \alpha = 135^\circ \end{array} \right. \quad (2)$$

where $LDEV(gy_{ab}) = LDEV$ at (a,b) location of 7×7 grid and gy_c is a gray metric of middle pixel. The upper LTP is filled with DTEC1 that is computed from Eq. (2) and using the measure of (\vec{f}_2) as provided below:

$$\vec{f}_2(a, gy_c) = \begin{cases} 1, & \text{if } (a \geq (\text{threshold} = 2)); \\ 0, & \text{if } (a < (\text{threshold})); \end{cases} \quad (3)$$

Similarly, from Eq. (2), lower LTP, DTEC2 have been measured by obtaining the given value of (\vec{f}_2) as follows:

$$\vec{f}_2(a, gy_c) = \begin{cases} 1, & \text{if } (a \geq (\text{threshold} = -2)); \\ 0, & \text{if } (a < (\text{threshold})); \end{cases} \quad (4)$$

The DTEC is derived from the Eqs. (2) - (4) are given below:

$$DTEC(IG(gy_c)) = \left[\begin{array}{l} DTEC1(IG(gy_c))|_{0^\circ}, DTEC1(IG(gy_c))|_{45^\circ}, DTEC1(IG(gy_c))|_{90^\circ}, DTEC1(IG(gy_c))|_{135^\circ}; \\ DTEC2(IG(gy_c))|_{0^\circ}, DTEC2(IG(gy_c))|_{45^\circ}, DTEC2(IG(gy_c))|_{90^\circ}, DTEC2(IG(gy_c))|_{135^\circ} \end{array} \right] \quad (5)$$

The DTEC coding is classified as two binary codes: upper LTP code as well as lower LTP code as similar to LTP. Practically, DLTerQEP allows the integration of tetra directional extremas of P=12-bit ($w=0 \dots 11$), and binary coding string generation for every binary pattern of LTP. By increasing the binomial weights for each DTEC LTP coding, a single DLTerQEP measures for particular pattern (7×7) characterizes the spatial structure of local pattern which can be defined using Eq. (6):

$$DLTerQEP_{\alpha, P} = \sum_{w=0}^{P-1} DTEC_{(\text{upper /lower})}, w2^w \quad (6)$$

From the entire image, each DTECLTP map presented is in the range of 0 to 4095 (0 to $2^P - 1$), as a result, the overall DTECLTP map is developed along with the previous value of 0 to 8191 (0 to $((2^P) - 1)$). The DLTerQEPs is totally varied from LBP method. It extracts the spatial association from the set of adjacent values from local regions including the directions allocated, and LBP is isolated using the correlation from middle

as well as neighboring pixels. It consumes the directional edge data on the basis of local extrema.

2.2. Edge feature extraction using Zernike Moments (ZM)

The clinical images of CT and MRI images include various features namely, textures, shape etc. Here, biomedical image retrieval method has the images acquired from diverse parts of human body. The total study of these images is important to provide clear distinction among them. Since it is emerged with local features, it is impossible to handle main factor an image, so that ZMs is used. It is assigned as a global descriptor for all medical images retrieval technique. This work employs the ZM in the form of shape descriptors as well as finds the rotation invariant due to the presence of Orthogonality behavior.

The ZMs is useful in capturing the essential features. The characteristic of orthogonality is seen from ZMs, which is more helpful to reach the adjacent measure of a redundant set of ZMs coefficients, hence, the moment values retrieved from various orders represents an exclusive and independent features of an image. It is known to be global feature descriptors since it has statistical distribution of pixel information within the minimum affected shape. Also, ZMs has been evaluated as the result of summation; thus, the effect of noise from a magnitude of ZMs coefficients is negotiated. The ZMs are considered to be an orthogonal moment which is obtained from the application of input image into complex orthogonal Zernike polynomials. In addition, ZMs of order u and reputed v of a expression $f(l,m)$ over a unit disk is represented as

$$Z_{uv} = \frac{u+1}{\pi} \iint_{l^2+m^2 \leq 1} f(l,m) Y_{uv}^*(l,m) dl dm \quad (7)$$

where u denoted a non-negative integer, v is an integer of $0 \leq |v| \leq u$, and $u-|v|=\text{even}$. The function of $Y_{uv}^*(l,m)$ is more complex in combining with Zernike orthogonal function $Y_{uv}(l,m)$ which is provided as:

$$Y_{uv}(l,m) = Y_{uv}(r,\theta) = R_{uv}(r) \exp(qv\theta) \quad (8)$$

where $= \sqrt{l^2+m^2}$, $\theta = \tan^{-1}\left(\frac{m}{l}\right)$ $0 \leq \theta \leq 2\pi$, $q = \sqrt{-1}$ The radial polynomial $R_{uv}(r)$ expressed as:

$$R_{uv}(r) = \sum_{s=0}^{(u-|v|)/2} (-1)^s \frac{(u-s)!}{s! \left(\frac{u+|v|}{2} - s\right)! \left(\frac{u-|v|}{2} - s\right)!} (r)^{u-2s} \quad (9)$$

The Zeroth order approximation of Eq. (9) is written as

$$Z_{uv} = \frac{2(u+1)}{\pi J^2} \sum_{p=0}^{J-1} \sum_{k=0}^{J-1} f(l_p, m_k) R_{uv}(r_{pk}) e^{-qv\theta_{pk}} \quad (10)$$

where (l_p, m_k) is a common coordinate location of corresponding pixel (p,k) which is gained from the application of coordinate transformation:

$$l_p = \frac{2p+1-J}{J\sqrt{2}}, m_k = \frac{2k+1-J}{J\sqrt{2}} \quad (11)$$

for all $p,k=0,1,2,\dots,J-1$. The exterior unit disk of ZMs computation provides an optimized notation for ZMs-relied image pattern matching problems. Also, the proposed technique of ZMs-based framework could not employ the tendency along with negative v , as it has $|Z_{u,v}| = |Z_{u,-v}|$.

2.3. Similarity measurement

In CBMIR technique, Euclidean distance is used to identify the resemblance between the given images. Thus, the distance from 2 images has been applied to determine the harmony of images. It is a compulsory distance value. It has been estimated with the help of Minkowski Distance expression by fixing p's rate as 2. For any 2 images l and m, the distance 'd' can be determined as follows:

$$d(l, m) = \sqrt[n]{\sum_{u=1}^n (l_u - m_u)^2} \quad (12)$$

2.4. GWO-DNN based classification

Generally, DNN is a feed forward network and it is an unsupervised pre-trained method by greedy layer wise training. Here, the data progresses from the input layer to output layer without looping function. The major benefits from DNN are the least number of possible missing values. DNN method applies only one layer in unsupervised pre-trained phase. This DNN distributes the classifier score $f(l)$ while predicting classes. Each input data instance can be represented as $l = [l_1, \dots, l_N]$. Typically, f is the function that contains an order of layers to calculate as given in Eq. (13):

$$Z_{uv} = l_u w_{uv}; Z_v = \sum_u Z_{uv} + b_v; X_v = g(Z_v) \quad (13)$$

where input layer is implied as l_u , output layer is indicated as l_v , and w_{uv} is the form parameters and $g(Z_v)$ recognizes the mapping function. Layer-wise propagation decays the classification result $f(l)$ with respect to relevance's r_u element to every input module l_u that supplies to classifier decision as explained in Eq. (14):

$$f(l) = \sum_u r_u, \quad (14)$$

where $r_u > 0$ denotes positive data maintaining the classified decision and $r_u < 0$ is the negative data; or else, it is known as neutral evidence, while the relevance attribute r_u is computed utilizing Eq. (15).

$$r_u = \sum_u \frac{z_{uv}}{\sum_u z_{uv}}. \quad (15)$$

The DNN is capable to examine the indefinite feature consistency of input. It gives the hierarchical feature learning manner. Thus, the higher level features are obtained from lower level features in a greedy layer wise unsupervised pre-trained data. So, the key intention of DNN is to manage the difficult function that is signifying higher level concept.

At the same time, the hyperparameter tuning of DNN also plays a major role in the classification performance. The training process of DNN has been influenced by the selection of hyperparameter configuration by the use of the different algorithms. In generally, effective adjustment of weights is based on the learning technique and the learning rate manages the difference in amplitude of the parameters. This paper addresses the challenging issue of hyperparameter configuration of DNN by the use of GWO algorithm.

The GWO is assumed to be a swarm intelligence relied method that resembles the dominant hierarchy as well as hunting methodology of grey wolves. In order to promote the leadership hierarchy, 4 kinds of grey wolves have been applied such as alpha (α), beta (β), delta (δ), and omega (ω). Also, there are 3 major phases involved in GWO and is listed as follows:

- Exploring the prey,
- surrounding prey,
- Attacking prey.

The fundamental GWO technique is projected in Algorithm 1. The GWO-DNN model is mainly employed to identify an optimized DNN topology, number of hidden layers, neurons, dropout possibility as well as activation function for all layers and optimized function of DNN. Hence, the result of every DNN topology is allocated under the application of sigmoid activation function and uniform function to initialize the kernel. The hyperparameter tuning of DNN using GWO algorithm will greatly improve the classifier performance.

Algorithm 1: GWO algorithm

Step 1: Population initialization of grey wolves $X_i (i = 1, 2, \dots, n)$

Step 2: Initialization of a, A and C

Step 3: Determine the fitness of all search agents

Step 4: X_α = optimal search agent

Step 5: X_β = near optimal search agent

Step 6: X_δ = third optimal best search agent

Step 7: if termination condition is not met do

Step 8: for every search agent do

Step 9: Updates the location of the existing search agent

Step 10: end for

Step 11: Updates a, A , and C

Step 12: Determine the fitness of every search agent

Step 13: Updates X_α, X_β , and X_δ

Step 14: end if

Step 15: return X_α

3. Performance Validation

3.1. Dataset used

To validate the results of proposed method, a standard NEMA CT images are applied that captures diverse parts of the human body [19]. It offers accurate data presentation to differentiate the images composed in entire representation, which is a global scale. The data has been compared to NEMA CT dataset which is provided in Table 1, comprising a set of 600 images with the pixel dimensions of 512*512. Besides, a set of ten classes were exist in the whole dataset.

Table 1. Dataset Description

Description	Values
Database	NEMA CT
Number of Images	600
Image Size	512*512
Number of Classes	10
Classes Distribution	54, 70, 66, 50, 15, 60, 52, 104, 60, 69

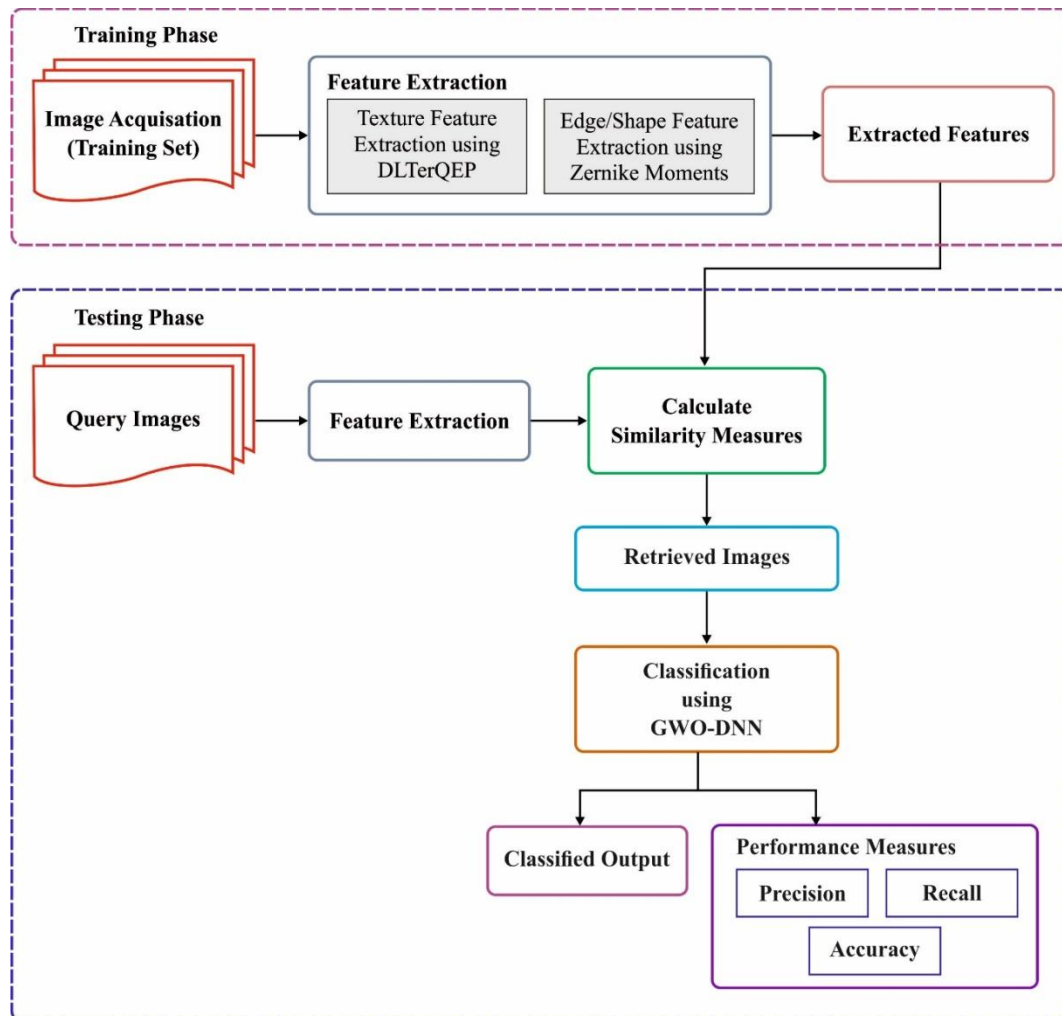


Figure 1. Overall Process of Proposed Method

3.2. Results Analysis

An extended process is created in the proposed technique as well as previous methods as depicted in Table 2. Figure. 2-4 exhibit the final outcome of different technique with respect to precision, recall and accuracy. By analyzing the result of proposed technique on the sample dataset in terms of precision, it is demonstrated in group of 3 methods as LTDP, LQEP and LMeP methodologies attains lower precision values of 8.97%, 8.93% and 8.91% respectively. Followed by, a better outcome is provided by the LDEP,

DLTerQEP and LDGP methods by reaching near precision metrics of 10.27%, 9.10% and 10.27%. At the same time, the LWP and LBDP technology offers reasonable as well as closer precision values of 31.03% and 32.57%. Similarly, the OFMM and PSO-SVM techniques offer a best classifying result by providing maximum precision value of 48.51% and 53.67%. But, the projected technique offers higher results by attaining optimized precision of 89.39%.

By calculating the classification outcome with respect to recall, it is appeared as a group of 4 methods such as DLTerQEP LTDP, LQEP and LMeP has provided inaccurate classifying result by reaching the measures of 16.68%, 16.59%, 16.55% and 16.66% respectively. Simultaneously, a slightly better outcome is provided the LDEP and LDGP methodologies by reaching closer identical recall values of 18.39% and 17.28%. As same as, the LWP and LBDP models offers manageable and identical recall values of 46.51% and 47.11%. Concurrently, the OFMM and PSO-SVM models provides near optimal classification result by providing a maximum recall value of 74.12% and 77.89%. Hence, the presented technique provided higher results by reaching optimized recall of 94.18%.

Table 2 Comparison of different models under diverse measures

Methods	Precision	Recall	Accuracy
GWO+DNN	89.39	94.18	93.73
PSO+SVM	53.67	77.89	65.38
OFMM	48.51	74.12	60.52
LBDP	32.57	47.11	40.61
LWP	31.03	46.51	38.54
LDEP	10.27	18.39	15.96
DLTerQEP	09.10	16.68	13.62
LDGP	09.05	17.28	13.51
LTDP	08.97	16.59	12.94
LQEP	08.93	16.55	12.85
LMeP	08.91	16.66	12.64

By relating the simulation outcome obtained from presented methods in terms of accuracy, it is referred that LTDP, LQEP and LMeP attains minimized accuracy of 12.94%, 12.85% and 12.64% respectively. Followed by, a slightly better result is derived from LDEP, DLTerQEP and LDGP techniques by reaching closer accuracy value of 15.96%, 13.62% and 13.51%. Concurrently, LWP as well as LBDP methods exhibit applicable and closer accuracy measures of 38.54% and 40.61%. Likewise, the OFMM and PSO-SVM frameworks offer adjacent optimal classification result by generating a higher accuracy value of 60.52% and 65.38% respectively. Therefore, the deployed methods offered good results by reaching the optimized accuracy value of 93.73%. By studying the above reported tables as well as figures, it is ensured that the proposed method offers qualified retrieval and classification function in various factors.

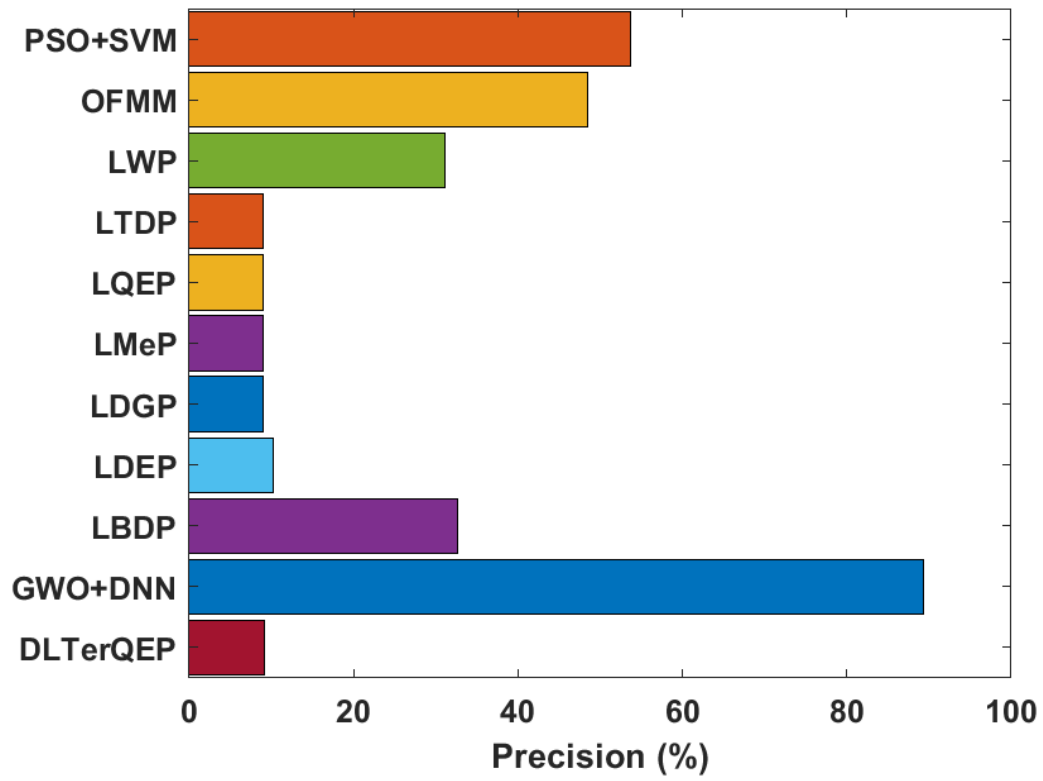


Figure 2. Precision analysis of diverse models

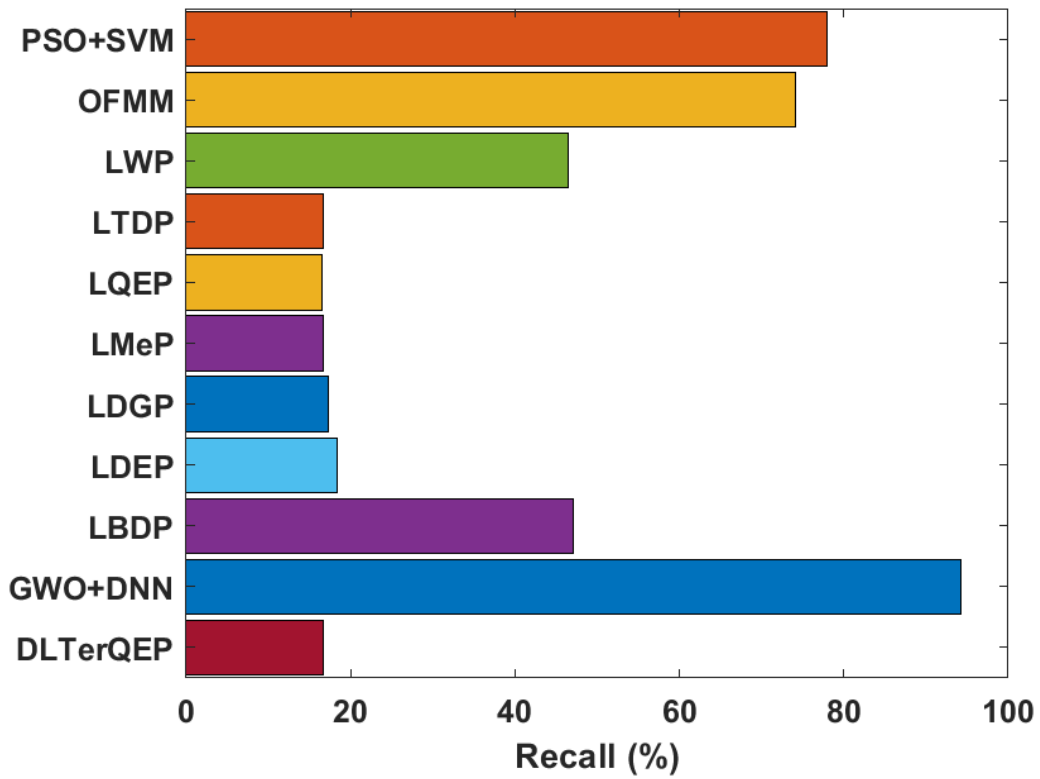


Figure 3. Recall analysis of diverse models

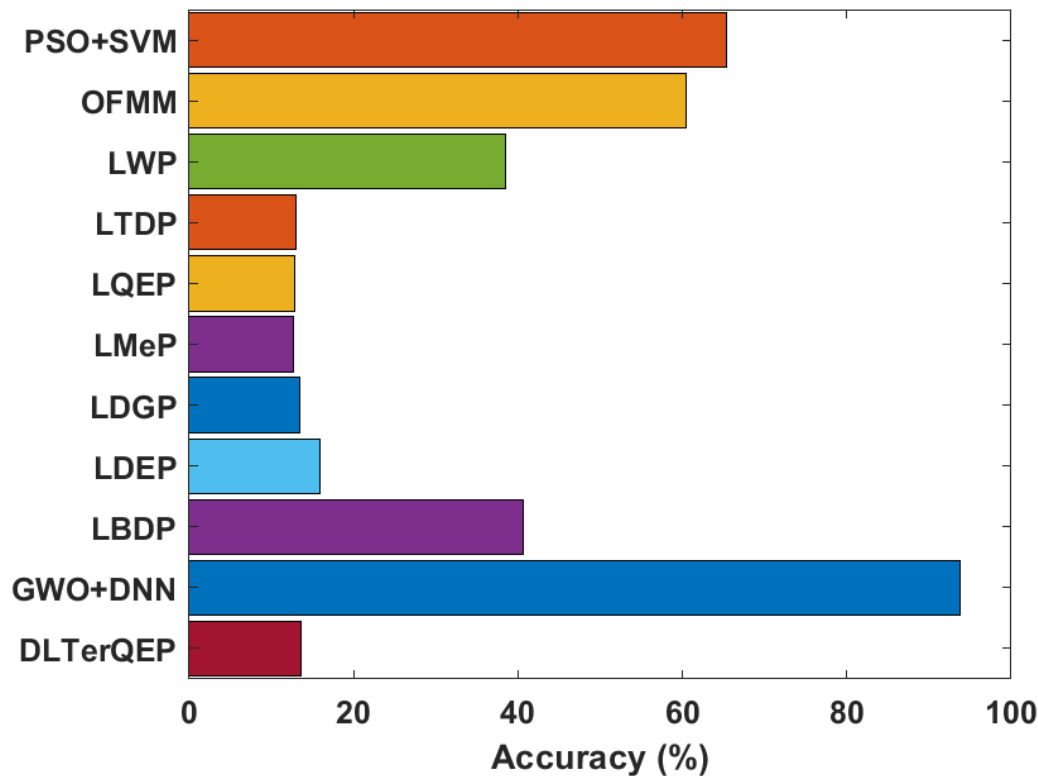


Figure 4. Accuracy analysis of diverse methods

4. Conclusion

For the effective retrieval and classification of medicinal images from huge databases, it is needed to develop an effective medical image retrieval and classification model. In this paper, a new medical image retrieval and classification model has been developed. The entire process is divided into two main phases namely training phase and testing phase. In the training phase, the input image is induced to feature extraction stage which involves an extraction of a set of two definite features like texture as well as edges. During the testing phase, the input query image undergo feature extraction process and attains a set of features exist in the image. Based on the similarity measure, the relevant images will be retrieved. After the retrieving of relevant images, GWO-DNN dependent image classification process is carried out. To validate the results of proposed method, a standard NEMA CT images are applied. The experimental results clearly portrayed the significance of the proposed model by attaining a maximum precision of 89.39%, recall of 94.18% and accuracy of 93.73%. The proposed model can be employed as an effective tool for real time medical diagnosis process.

References

- [1] Y. Rui, T.S. Huang, Image retrieval: current techniques, promising directions and open issues, *J. Vis. Commun. Image Representation* 10 (1999) 39–62.
- [2] A.W.M. Smeulders, M. Worring, S. Santini, A. Gupta, R. Jain, Content-based image retrieval at the end of the early years, *IEEE Trans. Pattern Anal. Mach. Intell.* 22 (2000) 1349–1380.
- [3] M. Kokare, B.N. Chatterji, P.K. Biswas, A survey on current content based image retrieval methods, *IETE J. Res.* 48 (2002) 261–271.
- [4] Y. Liu, D. Zhang, G. Lu, W.-Y. Ma, A survey of content-based image retrieval with high-level semantics, *Pattern Recogn.* 40 (2007) 262–282.
- [5] H. Muller, N. Michoux, D. Bandon, A. Geisbuhler, A review of content-based image retrieval systems in medical applications—Clinical benefits and future directions, *Int. J. Med. Inf.* 73 (2004) 1–23.

- [6] K.N. Manjunath, A. Renuka, U.C. Niranjan, Linear models of cumulative distribution function for content-based medical image retrieval, *J. Med. Syst.* 31 (2007) 433–443
- [7] F.S. Zakeri, H. Behnam, N. Ahmadinejad, Classification of benign and malignant breast masses based on shape and texture features in sonography images, *J. Med. Syst.* 36 (2010) 1621–1627.
- [8] G. Quellec, M. Lamard, G. Cazuguel, B. Cochener, C. Roux, Wavelet optimization for content-based image retrieval in medical databases, *J. Med. Image Anal.* 14 (2010) 227–241.
- [9] A.J. Traina, C.A. Castanon, C. Traina Jr, Multiwavemed: a system for medical image retrieval through wavelets transformations, in: *Proceedings of the 16th IEEE Symposium on Computer-Based Medical Systems*, New York, USA, 2003, pp. 150–155.
- [10] J.C. Felipe, A.J. Traina, C. Traina Jr, Retrieval by content of medical images using texture for tissue identification, in: *Proceedings of the 16th IEEE Symposium on Computer-Based Medical Systems*, New York USA, 2003, pp. 175–180.
- [11] D. Unay, A. Ekin, R.S. Jasinschi, Local structure-based region-of interest retrieval in brain MR images, *IEEE Trans. Inf. Technol. Biomed.* 14 (2010) 897–903.
- [12] L. Sørensen, S.B. Shaker, M. de Bruijne, Quantitative analysis of pulmonary emphysema using local binary patterns, *IEEE Trans. Med. Imaging* 29 (2010) 559–569.
- [13] S.H. Peng, D.H. Kim, S.L. Lee, M.K. Lim, Texture feature extraction based on uniformity estimation method for local brightness and structure in chest CT images, *Comput. Biol. Med.* 40 (2010) 931–942.
- [14] A. Qudus, O. Basir, Semantic image retrieval in magnetic resonance brain volumes, *IEEE Trans. Inf. Technol. Biomed.* 16 (2012) 348–355.
- [15] S. Murala, Q.M.J. Wu, Local ternary co-occurrence patterns: a new feature descriptor for MRI and CT image retrieval, *Neurocomputing* 119 (2013) 399–412.
- [16] S. Murala, Q.M.J. Wu, Local mesh patterns versus local binary patterns: biomedical image indexing and retrieval, *IEEE J. Biomed. Health. Inf.* 18 (2014) 929–938.
- [17] S. Murala, Q.M.J. Wu, MRI and CT image indexing and retrieval using local mesh peak valley edge patterns, *Signal Process. Image Commun.* 29 (2014) 400–409
- [18] S.R. Dubey, S.K. Singh, R.K. Singh, Local diagonal extrema pattern: a new and efficient feature descriptor for CT image retrieval, *IEEE Signal Process Lett.* 22 (2015) 1215–1219.

Authors



C.Ashok kumar, received MSc (IT) degree from Madras University and M.Phil degree from Bharathidasan University, India. He joined in the Annamalai University in the year 2005. At present he is working in the Department of Computer Science, Dr.MGR Arts & Science College, Villupuram. He has almost 14 years of teaching experience. He is currently pursuing Ph.D degree in the Department of Computer and Information Science, Annamalai University. His research interests include Pattern Recognition and Image Retrieval.



S.Sathiamoorthy, received B.Sc degree in Physics from University of Madras, M.C.A degree from Bharathidasan University and M.Phil as well as Ph.D. from Annamalai University, India. In the year 2001, he joined in the Department of Computer Science and Engineering, Annamalai University and also served in the Computer Science and Engineering Wing of Directorate of Distance Education and Department of Computer and Information Science, Annamalai University. At present, he is Assistant Director (Controller of Examinations), Tamil Virtual Academy, Information Technology Department of Tamil Nadu Government, India. He has almost 19 years of teaching experience. Currently he is working on Pattern recognition, Pattern analysis, Image retrieval and classification. His research interests include Machine learning algorithms and Medical image analysis. He has published more than 30 papers in various International journals and more than 20 papers in National and International conferences. He has been on the reviewing and editorial board of many reputed journals.